Electronic Supplementary Material (ESI) for Molecular Systems Design & Engineering.

Supplementary material for

Isolating the effects of gate layer permeability and sorbent density on the performance of solute-selective polymeric ion pumps

Jonathan Aubuchon Ouimet, Alexander W. Dowling, William A. Phillip

Department of Chemical and Biomolecular Engineering, University of Notre Dame, Notre Dame, Indiana 46556, United States

* To whom correspondence should be addressed: wphillip@nd.edu

Table of Contents

1.0 GitHub Link – Analysis Codes

The code used for the analysis can be accessed through the following GitHub Repository.

2.0. Unloading Stage: Unsteady State Mass Balance Solution

At the onset of the unloading stage, ligands within the sorbent layer release bound solute molecules and diffusion drives the transport of solute out of the sorbent. The time-dependent concentration profile of solute in the sorbent layer can be determined by solving Equation 1.

$$\frac{\partial \mathrm{c^s}}{\partial t} = D^s \frac{\partial^2 \mathrm{c^s}}{\partial \mathrm{z}^2} \qquad 1$$

$\mathrm{c^s}$ and $\mathrm{D^s}$ are the concentration and diffusion coefficient of the solute in the sorbent layer, respectively, t is the time, and z defines the coordinate system across the thickness of the sorbent layer.

Within this work, we consider the effect of an imperfect gate layer that allows solute to diffuse both upstream into the feed solution and downstream into the receiving solution during the unloading stage. This physical phenomenon is described using a boundary condition that quantifies the flux of solute at the interface between the gate and sorbent layers, at $\mathrm{z} = 0$, Equation 2.

$$-\mathrm{D^s} \frac{\partial \mathrm{c^s}}{\partial \mathrm{z}}|_{\mathrm{z}=0} = -\mathrm{B}(\mathrm{c^s}|_{z=0} - \mathrm{c_f}) \qquad 2$$

$\mathrm{c^s}|_{z=0}$ is the concentration of solute at the interface between the gate and sorbent layers, $\mathrm{c_f}$ is the concentration of solute in the feed solution, and B is the solute permeability coefficient for the gate layer. This form of the equation implies that the gate layer is at pseudo-steady state. The receiving solution, $\mathrm{c_p}$, is assumed to be well mixed and free of solute, Equation 3.

$$\mathrm{c^s}|_{z=L} = \mathrm{c_p} = 0 \qquad 3$$

The initial condition required to solve Equation 1 is defined by the concentration profile at the end of the previous loading stage, Equation 4.

$$c^s(z)|_{t=0} = \underbrace{c^s(z)|_{t=t_l}}_{\substack{end\ of \\ loading}}. \quad 4$$

The feed concentration and the thickness of the sorbent layer are used to non-dimensionalize the concentration of solute and the coordinate system, respectively. The diffusion time, $t_D = L^2/D^s$, emerges naturally to non-dimensionalize the time, Equation 5.

$$\mathbb{c} = \frac{c^s}{c_f}, \xi = \frac{z}{L}, \tau = \frac{t}{L^2/D^s} \quad 5$$

As such, the governing equation (Equation 6), boundary conditions (Equations 7-8), and initial condition (Equation 9) are rewritten.

$$\frac{\partial \mathbb{c}}{\partial \tau} = \frac{\partial^2 \mathbb{c}}{\partial \xi^2} \quad 6$$

$$-\frac{\partial \mathbb{c}}{\partial \xi} = -\frac{BL}{D^m}\left(\mathbb{c}|_{\xi=0} - 1\right) = -Bi\left(\mathbb{c}|_{\xi=0} - 1\right) \quad 7$$

$$\mathbb{c}|_{\xi=1} = 0 \quad 8$$

$$\mathbb{c}(\xi)|_{\tau_{ul}=0} = \mathbb{c}(\xi)|_{\tau=\tau_l} \quad 9$$

The Biot number, Bi, appears in the upstream boundary condition (Equation 7) due to this dimensional analysis. The Biot number provides a ratio of the resistance to permeation offered by the sorbent layer relative to the gate layer.

The partial differential equation is solved by writing the concentration within the sorbent matrix as the sum of a steady state, $\mathbb{c}_{ss}$, and transient, $\mathbb{c}_t$, component, Equation S1.

$$\mathbb{c} = \mathbb{c}_{ss} + \mathbb{c}_t \quad S1$$

The governing equation and boundary conditions for the steady state component are not dependent on the time. Therefore, Equations 6-8 simplify to Equations S2-S4. The differential equation is solved to determine the steady state solution (Equation S5).

$$0 = \frac{d^2 \mathbb{c}_{ss}}{d\xi^2} \quad \text{S2}$$

$$-\frac{\partial \mathbb{c}_{ss}}{\partial \xi} = -\mathrm{Bi}\left(\mathbb{c}_{\mathrm{ss}}|_{\xi=0} - 1\right) \quad \text{S3}$$

$$\mathbb{c}_{\mathrm{ss}}|_{\xi=1} = 0 \quad \text{S4}$$

$$\mathbb{c}_{ss} = \frac{Bi}{Bi+1}(1-\xi) \quad \text{S5}$$

For an impermeable gate layer (i.e., $Bi = 0$), the steady state solution corresponds to all the solute diffusing out of the membrane. For an imperfect gate layer (i.e., $Bi > 0$), the steady-state concentration profile is related to the resistance between the gate layer and the sorbent layer.

The transient solution is defined by the following partial differential equation (Equation S6) and boundary conditions (Equation S7 and S8).

$$\frac{\partial \mathbb{c}_{\mathrm{t}}}{\partial \tau} = \frac{\partial^2 \mathbb{c}_t}{\partial \xi^2} \quad \text{S6}$$

$$\frac{\partial \mathbb{c}_t}{\partial \xi} = \mathrm{Bi}\ \mathbb{c}_t|_{\xi=0} \quad \text{S7}$$

$$\mathbb{c}_{\mathrm{t}}|_{\xi=1} = 0 \quad \text{S8}$$

The partial differential equation is solved using separation of variables, Equation S9.

$$\mathbb{c}_t = G(\tau)F(\xi) = \sum_{n=1}^{\infty} A_n e^{-\sigma_n^2 \tau}[B_n \cos(\sigma_n \xi) + C_n \sin(\sigma_n \xi)] \quad \text{S9}$$

The boundary conditions are applied to simplify the coefficients, Equation S10.

$$\mathbb{c}_t = \sum_{n=1}^{\infty} A'_n e^{-\sigma_n^2 \tau}\{\cos(\sigma_n \xi) + \frac{Bi}{\sigma_n}\sin(\sigma_n \xi)\} \quad \text{S10}$$

The integration constants, A'_n (Equation S11), are defined by the previous loading stage concentration profile, $\underbrace{\mathbb{c}_t|_{\tau_{ul}=0}}_{\substack{start\ of \\ unloading}} = \underbrace{\mathbb{c}_t|_{\tau=\tau_l}}_{\substack{end\ of \\ loading}}$ and the eigenvalues, σ_n (Equation S12).

$$A'_n = A_n B_n = \frac{\int_0^1 \left\{\mathbb{c}_t|_{\tau=\tau_l}\right\}\left\{\cos(\sigma_n \xi) + \frac{Bi}{\sigma_n}\sin(\sigma_n \xi)\right\} d\xi}{\int_0^1 \left\{\cos(\sigma_n \xi) + \frac{Bi}{\sigma_n}\sin(\sigma_n \xi)\right\}^2 d\xi} \quad \text{S11}$$

$$-\sigma_n \cot(\sigma_n) = Bi \quad \text{S12}$$

Together, the steady state and transient solutions provide the time-varying concentration profile of the unloading stage, Equation S13.

$$\mathbb{c} = \frac{Bi}{Bi+1}(1-\xi) + \sum_{n=1}^{\infty} A'_n e^{-\sigma_n^2 \tau}\{\cos(\sigma_n \xi) + \frac{Bi}{\sigma_n}\sin(\sigma_n \xi)\} \quad \text{S13}$$

3. *Supplementary Figures*

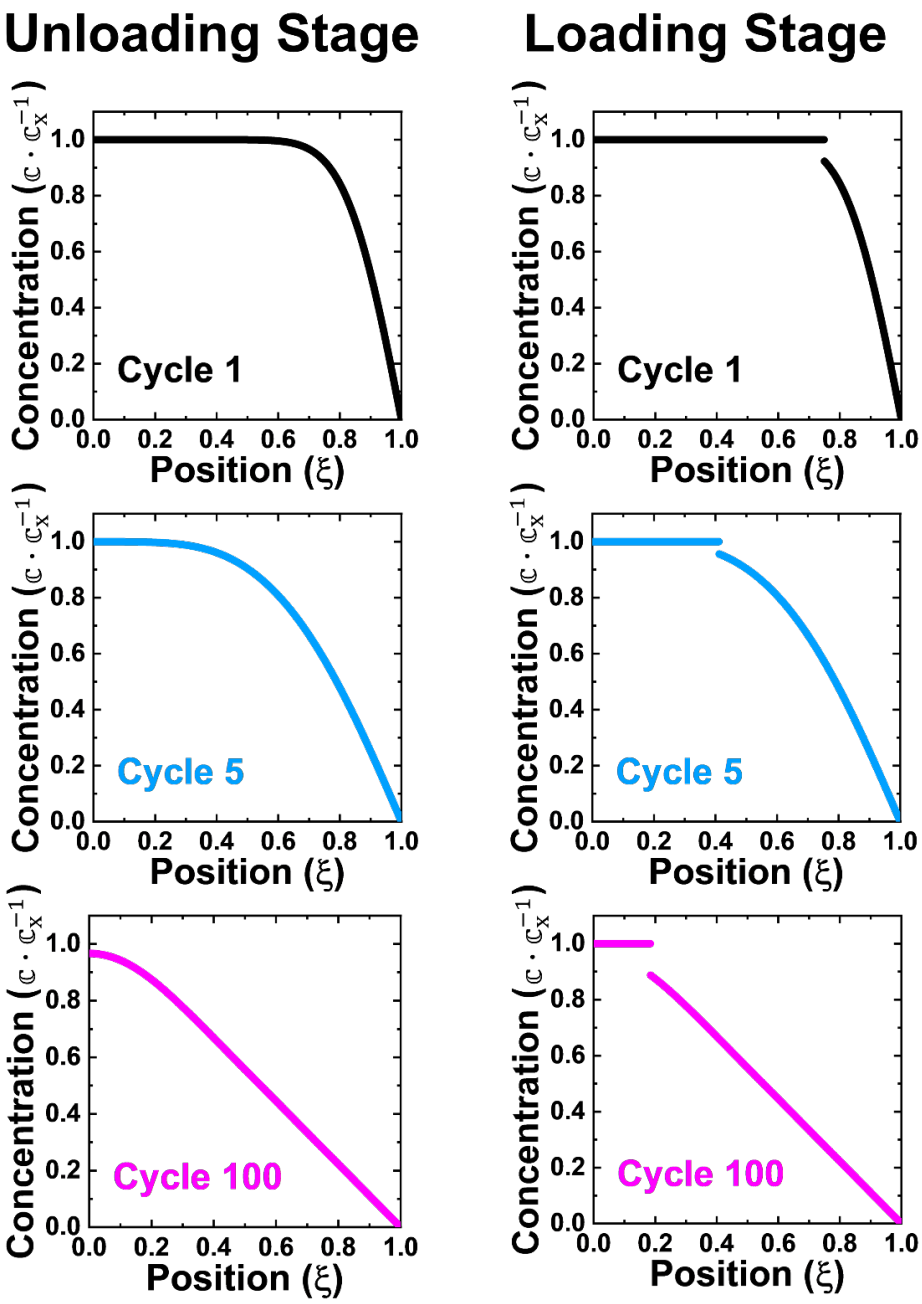

Figure S1: Solute concentration profiles for a $\mathrm{Bi} = 0$ system. The concentration profile after 1, 5 and 100 unloading and loading cycles are plotted for systems where $\mathbb{c}_x = 10$ and $\mathrm{Bi} = 0$. The systems are operating at dimensionless unloading time, τ_{ul}, 0.01 and loading time, τ_l, 0.0125. The simulations were initialized with a saturated sorbent layer $\left(\frac{\mathbb{c}}{\mathbb{c}_x} = 1\right)$.

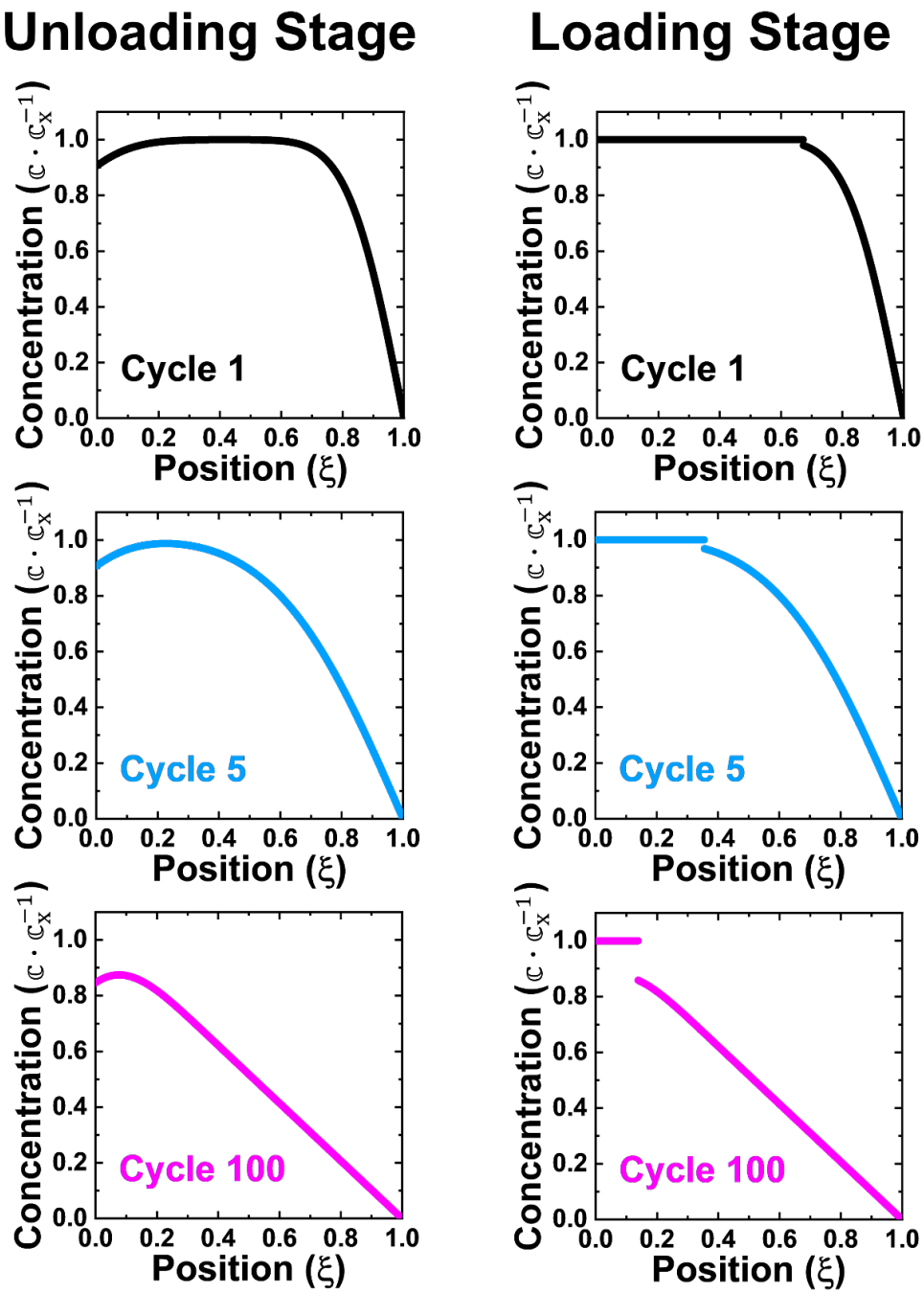

Figure S2: Solute concentration profiles for a $\mathrm{Bi} = 1$ system. The concentration profile after 1, 5 and 100 unloading and loading cycles are plotted for systems where $\mathbb{c}_x = 10$ and $\mathrm{Bi} = 1$. The systems are operating at dimensionless unloading time, τ_{ul}, 0.01 and loading time, τ_l, 0.0125. The simulations were initialized with a saturated sorbent layer $\left(\frac{\mathbb{c}}{\mathbb{c}_x} = 1\right)$.

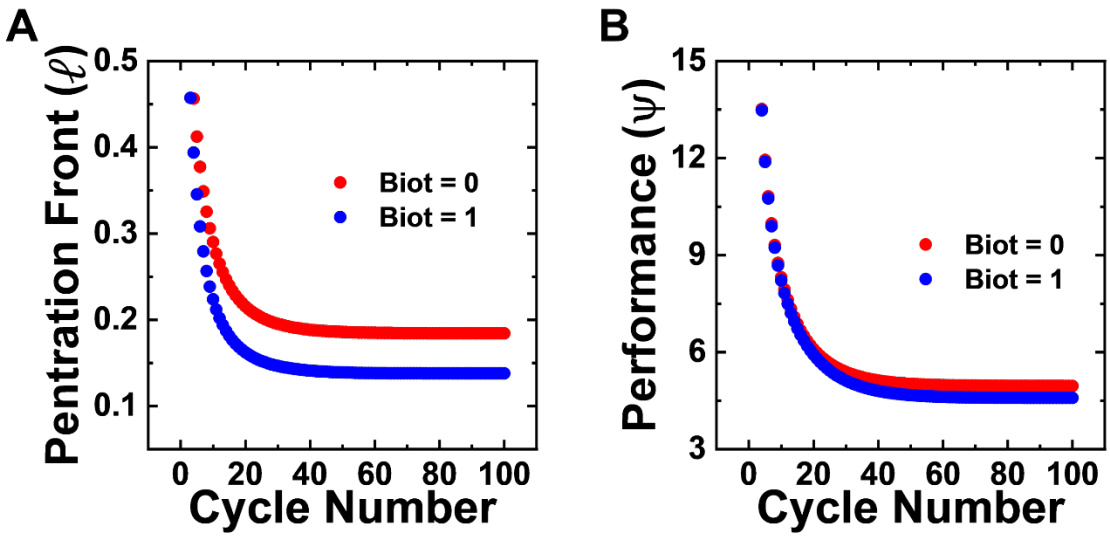

Figure S3: The change in the **(A)** penetration front and **(B)** performance with increasing cycles. While the flux of solute into the sorbent layer during the loading stage balancing the flux of solute out of the sorbent layer during the unloading stage is used to assess PSS, the penetration front and performance corroborate that a system has reached pseudo-steady state. Simulations are initialized with a saturated sorbent layer operating at nondimensional unloading time, τ_{ul}, 0.01 and loading time, τ_l, 0.0125. Red data points correspond to a system with $\mathrm{Bi} = 0$. Blue data points correspond to a system with $\mathrm{Bi} = 1$. The penetration front and performance converge to a constant value as the systems approach pseudo-steady state.

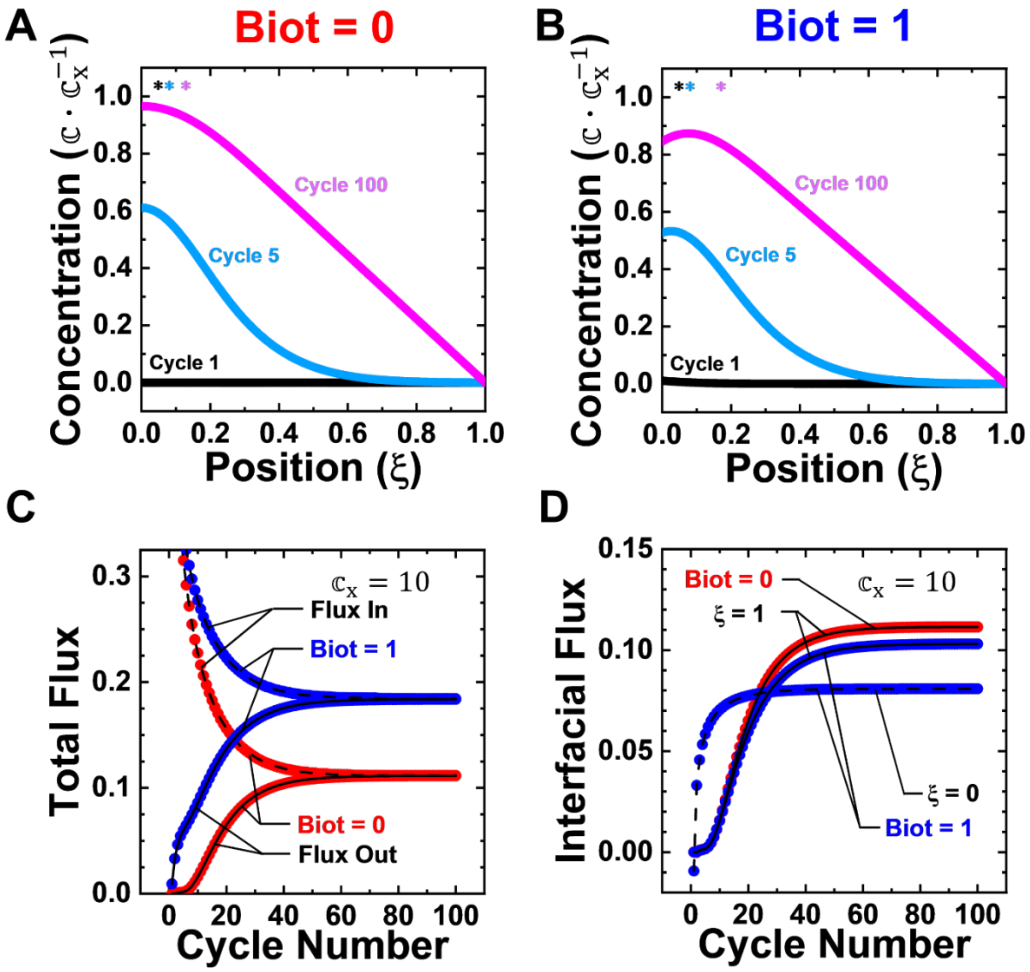

Figure S4: Mathematical evaluation of the approach to pseudo-steady state for simulations initialized with an empty sorbent layer $\left(\frac{\mathbb{c}}{\mathbb{c}_x} = 0\right)$. The concentration profile after 1, 5 and 100 unloading cycles are plotted for systems [**(A)** $\mathrm{Bi} = 0$ and **(B)** $\mathrm{Bi} = 1$] operating at dimensionless unloading time, τ_{ul}, 0.01 and loading time, τ_l, 0.0125. The location of the penetration fronts of the loading stage are indicated with asterisks. **(C)** The total flux of solute entering (Flux In) and exiting (Flux Out) the sorbent layer for the $\mathrm{Bi} = 0$ (red data points) and $\mathrm{Bi} = 1$ (light blue data points) systems. **(D)** The total flux out is broken into individual components for $\mathrm{Bi} = 0$ (red) and $\mathrm{Bi} = 1$ (light blue) systems. The data points indicated by $\xi = 1$ correspond to the flux of solute into the receiving solution. The data points indicated by $\xi = 0$ correspond to the flux of solute into the upstream reservoir.

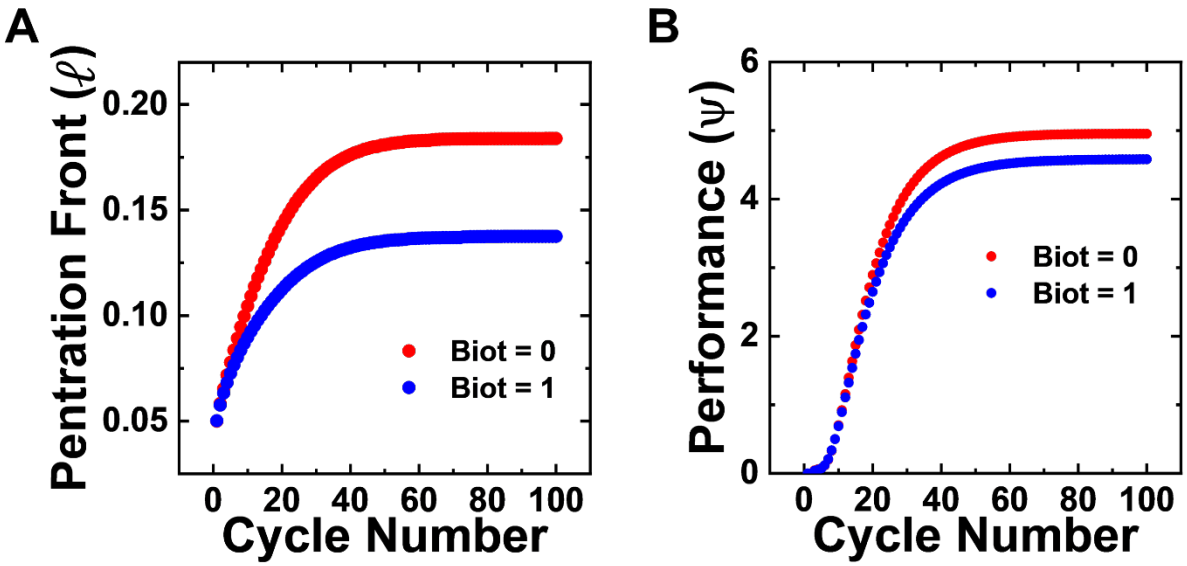

Figure S5: The change in the **(A)** penetration front and **(B)** performance with increasing cycles. While the flux of solute into the sorbent layer during the loading stage balancing the flux of solute out of the sorbent layer during the unloading stage is used to assess PSS, the penetration front and performance corroborate that a system has reached pseudo-steady state. Simulations are initialized with an empty sorbent layer operating at nondimensional unloading time, τ_{ul}, 0.01 and loading time, τ_l, 0.0125. Red data points correspond to a system with $\mathrm{Bi} = 0$. Blue data points correspond to a system with $\mathrm{Bi} = 1$. The penetration front and performance converge to a constant value as the systems approach pseudo-steady state.

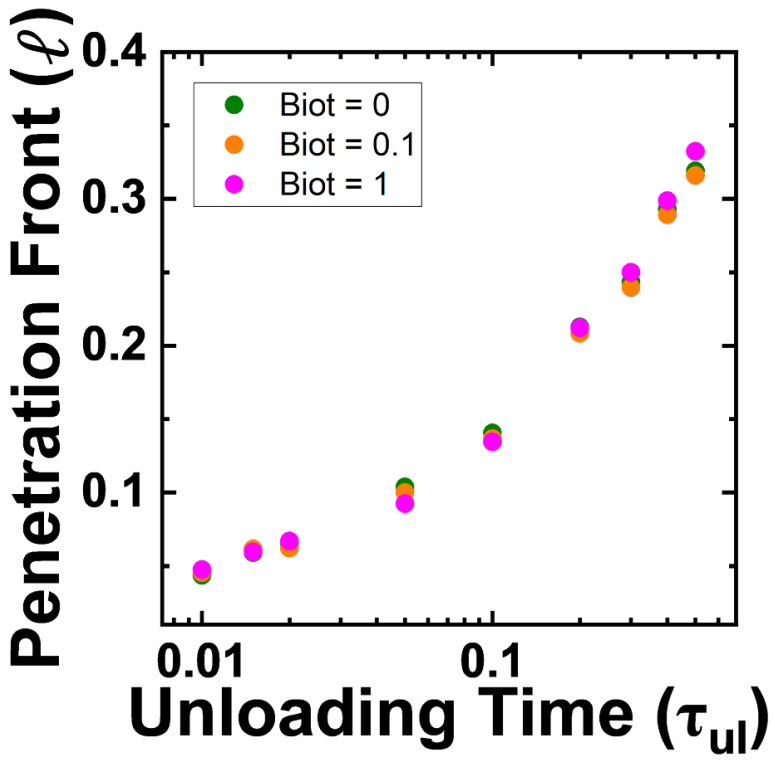

Figure S6. The penetration front is plotted as a function of the unloading time for systems where $\mathbb{c}_x = 10$ and $Bi = 0, 0.1$, or 1. The penetration front is independent of the Biot number at fixed unloading times.

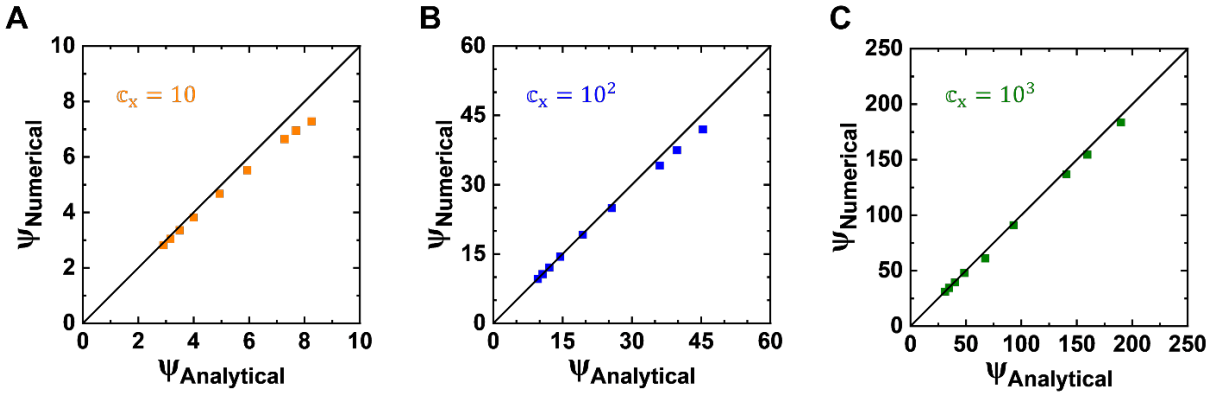

Figure S7. A parity plot of the numerical (y-axis) and analytical (x-axis) performances. Systems with sorbent densities of **(A)** 10, **(B)** 100 and **(C)** 1000 are presented. The black 45-degree line is used to indicate solutions that are equal.

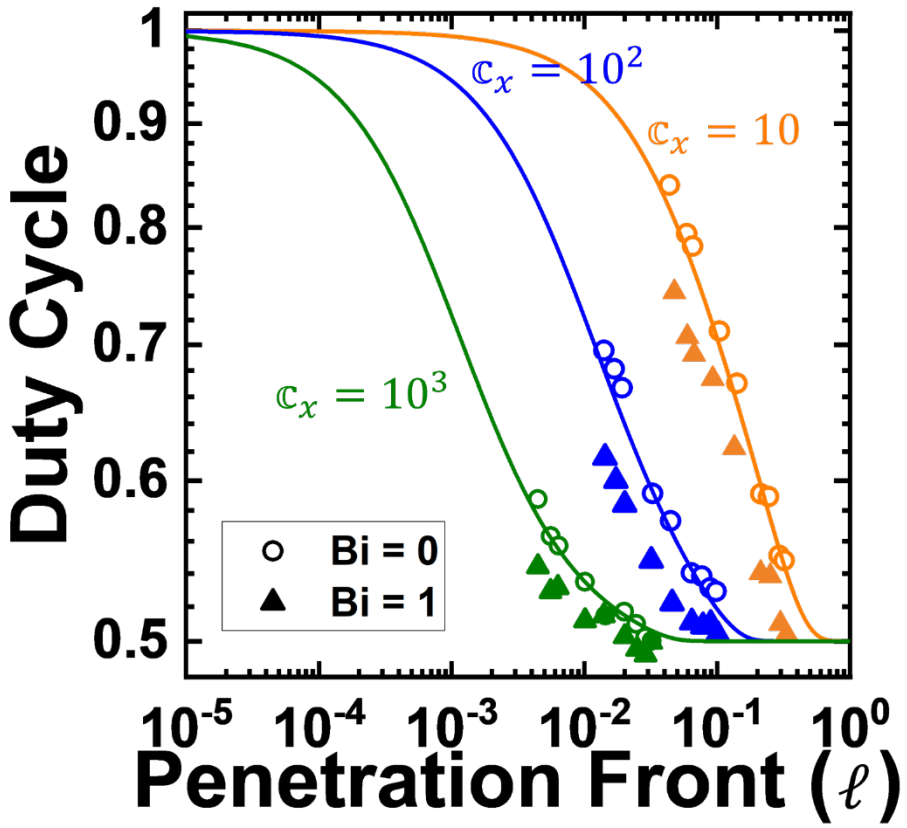

Figure S8. The optimal process operating conditions (i.e., τ_{ul} and τ_l) converge with increasing sorbent densities. The solid lines correspond to the analytical solutions of systems with impermeable gate layers and sorbent densities of 10 (orange), 100 (blue) and 1000 (green). For each sorbent density, open circles and filled triangles correspond to the numerical solution of systems with Biot numbers of 0 and 1, respectively.

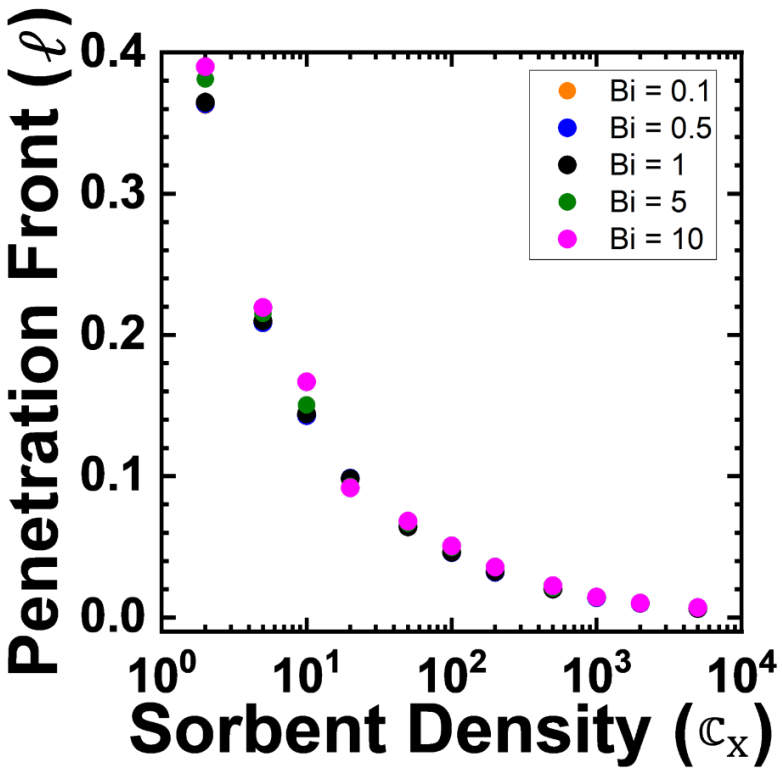

Figure S9. For an optimized system operating at $\tau_{ul} = 0.1$, the penetration front is plotted at varying sorbent densities for five different Biot numbers. The penetration front is independent of the Biot number for sufficiently high $\mathbb{c}_x$.

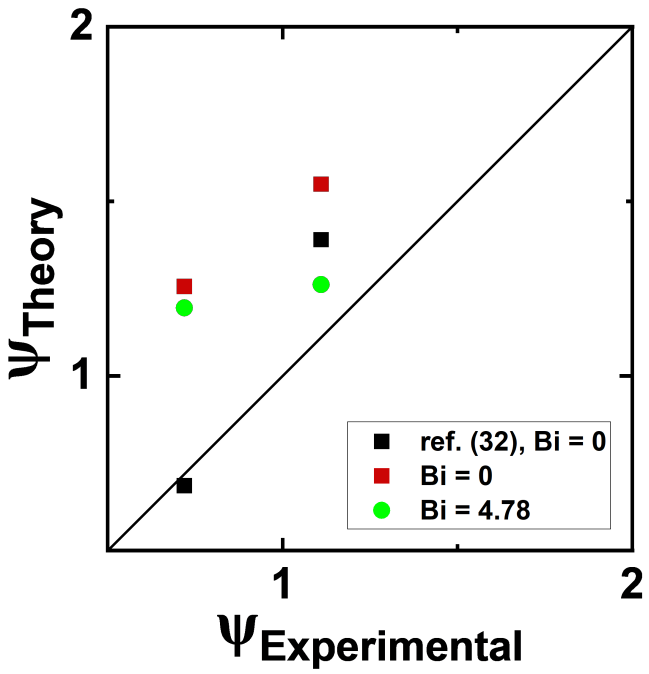

Figure S10. A parity plot comparing the experimental performance of polymeric ion pumps from literature and the performance predicted by the numerical solver. The black squares correspond to the analytical solution derived from an impermeable gate layer.[1] The red squares correspond to the numerical performance of a system with an impermeable gate layer during the unloading stage. The green circles correspond to the performance of the system after material properties define the permeability of the gate layer (i.e., Bi = 4.78).